

# A Study of a Flapping Flag in Viscoelastic Fluids and its Implications for Micro-Scale Swimming in Biofluids

by

Batya A. Fellman

Submitted to the Department of Mechanical Engineering  
in partial fulfillment of the requirements for the degree of

Bachelor of Science in Mechanical Engineering

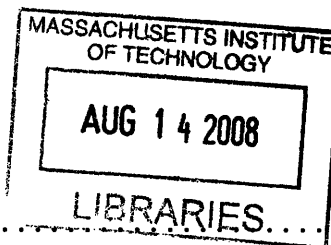
at the

MASSACHUSETTS INSTITUTE OF TECHNOLOGY

June 2008

© Batya A. Fellman 2008. All rights reserved.

The author hereby grants to MIT permission to reproduce and distribute publicly paper and electronic copies of this thesis document in whole or in part.



Author .

.....  
Department of Mechanical Engineering  
May 9, 2008

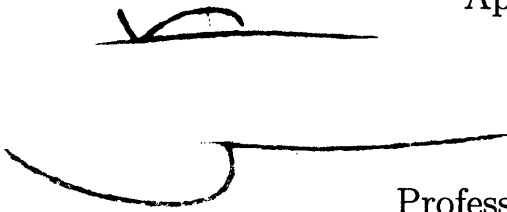
Certified by ...

.....  
Anette Hosoi  
Associate Professor of Mechanical Engineering  
Thesis Supervisor

Certified by:

.....  
Sunghwan Jung  
Applied Mathematics Instructor  
Thesis Supervisor

Accepted by

  
.....  
John H. Lienhard V  
Professor of Mechanical Engineering  
Chairman, Undergraduate Thesis Committee

# A Study of a Flapping Flag in Viscoelastic Fluids and its Implications for Micro-Scale Swimming in Biofluids

by

Batya A. Fellman

Submitted to the Department of Mechanical Engineering  
on May 9, 2008, in partial fulfillment of the  
requirements for the degree of  
Bachelor of Science in Mechanical Engineering

## Abstract

Biological cells and organisms employ a different method of propulsion when in viscous, viscoelastic fluids rather than Newtonian fluids. By studying the dynamics of a flag under a flow of a viscoelastic fluid, we hope to better understand the swimming dynamics in these biological fluids. A slender polysiloxane rod was placed in a rotating annulus filled with a cetyl pyridinium chloride micellar solution and also with a xanthan gum solution. Flapping of the rod was observed with the micellar solution for Weissenberg numbers greater than 1, where elastic forces in the fluid dominated the elastic force in the flag. Flapping was not observed in the xanthan gum for Weissenberg numbers up to 250, where the elastic force in the flag dominated the elastic force in the fluid. The observation of a flapping flag in a viscoelastic fluid indicates that, unlike in a Newtonian fluid, the polymers in the fluid can interact with an elastic body to cause a flapping motion which may indicate why the swimming dynamics of sperm change with their fluid environment.

Thesis Supervisor: Anette Hosoi  
Title: Associate Professor of Mechanical Engineering

Thesis Supervisor: Sunghwan Jung  
Title: Applied Mathematics Instructor

## Acknowledgments

I would like to graciously acknowledge the patience and dedication of Dr. Sunghwan “Sunny” Jung, without whom this project would not have been completed. I would also like to thank Professor Anette “Peko” Hosoi for all her help and guidance over the course of this research and the past few years. Additionally I would like to thank Matthieu Varagnat for his assistance with the micellar fluid, as well as Dr. Pedro Reis and Tony Yu for their insightful conversations.

# Contents

<b>1</b>	<b>Introduction</b>	<b>9</b>
<b>2</b>	<b>Background</b>	<b>12</b>
2.1	Newtonian and Non-Newtonian Fluids . . . . .	12
2.2	Critical Dimensionless Parameters . . . . .	13
2.2.1	Reynolds Number . . . . .	13
2.2.2	Deborah Number . . . . .	13
2.2.3	Weissenberg Number . . . . .	14
2.3	Viscoelastic Model . . . . .	15
<b>3</b>	<b>Experimental Methods</b>	<b>17</b>
3.1	Experiment Design . . . . .	17
3.2	Fluids Tested: Properties and Structure . . . . .	19
3.2.1	Xanthan Gum . . . . .	19
3.2.2	Micellar Fluid . . . . .	19
3.3	Flag Material and Composition . . . . .	21
3.4	Experimental Procedure . . . . .	22
<b>4</b>	<b>Results and Discussion</b>	<b>24</b>
4.1	Experimental Geometry and Dimensionless Groups . . . . .	24

4.2	Experimental Range of Parameters . . . . .	25
4.3	Flapping Image Analysis . . . . .	26
4.4	Flapping Behavior in Xanthan Gum and Micellar Fluid . . . . .	27
4.5	Flapping Frequencies in Micellar Fluid . . . . .	28
4.6	Bending Number: Dimensional Analysis of the Flapping . . . . .	30
4.7	Frequency Dimensional Analysis . . . . .	33
<b>5</b>	<b>Future Work</b>	<b>34</b>
<b>6</b>	<b>Conclusion</b>	<b>35</b>

# List of Figures

1-1	Depending on their environment, sperm adapt different dynamics. (a) Symmetrical beat pattern of activated sperm. (b) Asymmetric beat pattern of hyperactivated sperm. (c) Hyperactivated sperm in highly viscous and viscoelastic fluid (polyacrylamide). [6] . . . . .	11
3-1	The experimental setup consists of a stationary flag subjected to a flow by a rotating annulus. As the rotation rate is controlled, the motion of the flag in the flow is observed. . . . .	18
3-2	An overhead schematic of the experimental setup. . . . .	18
3-3	The molecular structure of the xantham gum polysaccharide [3] . . . . .	20
3-4	As the volume fraction of the surfactant molecule increases, the state of the solution changes [2] . . . . .	21
3-5	Image of the experimental setup. . . . .	22
4-1	Image sequence of the flag in a flow of 1.2rad/s. The red outline notes the position of the flag in the first frame. . . . .	28
4-2	As the Weissenberg number increases there is a clear linear relation with the flapping frequency. . . . .	29
4-3	For a flag placed 2.5 cm from the bottom of the channel, as the rate of rotation increases, so does the rate at which the tip of the flag is displaced. . . . .	30

4-4	Schematic showing the critical parameters on the flag. . . . .	31
6-1	Flapping was observed in the micellar fluid over a range of Weissenberg numbers, however no flapping was observed in the xanthan gum in this experiment.	36

# List of Tables

3.1 CPyCl/NaSal Fluid Properties at Varying Temperatures . . . . .	21
--	----

# Chapter 1

## Introduction

Fundamentally, microscopic organisms employ a different method of propulsion than large organisms. These large organisms, such as fish, swim at high Reynolds numbers where inertial forces dominate and at the simplest level can move forward by pushing fluid backwards in a reciprocal motion. In fact, by employing flapping dynamics, fish can lower their required energetic output through exploiting the vortices produced from the flapping motion. Microorganisms living at low Reynolds numbers ( $Re \ll 1$ ) essentially have no inertia and therefore cannot use this reciprocal motion, since they would just return to the same place as they started. Taylor was able to show through modeling a waving sheet that even in the absence of inertia, these objects could still self-propel in highly viscous fluids [7].

Since the majority of organisms on Earth are at microscopic level and there is a current trend towards design for the micro and nano-scales, understanding the propulsion at low Reynolds numbers is becoming increasingly important. There recently has been detailed research on low Reynolds swimmers in Newtonian fluids, especially in regards to the dynamics of undulating rods, rotating helices, and Purcell's swimmer, the simplest swimmer to move along its axis. However, less has been resolved in regards to the propulsion of these low Reynolds swimmers in non-Newtonian fluids which is closer to real life since many biofluids,

such as mucus and cytoplasm, are viscoelastic and non-Newtonian.

These microorganisms employ different methods of propulsion in different fluidic environments. The highly viscoelastic behavior of mucus in the female reproductive tract induces a change in the spermatozoa's waveform as seen in figure 1. Notably when the hyperactivated sperm were placed in a mucus made of polyacrylamide, their swimming dynamics changed to adapt to this new environment by straightening their tails and allowing them to swim faster [6].

Experimentally we seek to understand why the dynamics of microorganisms and cells such as the spermatozoa change upon interaction with highly viscoelastic fluids. By creating a physical model of a flag, which can emulate the flagellum, and inducing a flow in a viscoelastic fluid, the dynamics of the flag can be observed. Based on the motion of the flag in this fluid flow, insight can be made as to the locomotion of microorganisms in these highly non-Newtonian environments.

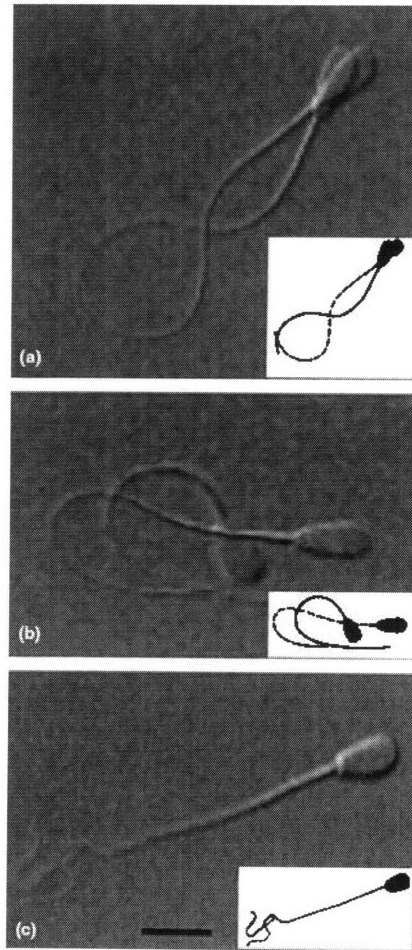


Figure 1-1: Depending on their environment, sperm adapt different dynamics. (a) Symmetrical beat pattern of activated sperm. (b) Asymmetric beat pattern of hyperactivated sperm. (c) Hyperactivated sperm in highly viscous and viscoelastic fluid (polyacrylamide). [6]

# Chapter 2

## Background

### 2.1 Newtonian and Non-Newtonian Fluids

When polymers are introduced into a standard Newtonian fluid, such as water or glycerol, the fluid is then called viscoelastic and takes on a so-called "non-Newtonian" behavior. The viscoelastic nature of the fluid arises from the property that it retains a magnitude of elasticity and can in some capacity return to its original shape. The properties of the fluid are therefore time-dependent and rely on how the polymers within the fluid deform under stress. Additionally, this fluid experiences a nonlinear or non-Newtonian viscosity. Unlike a Newtonian fluid that has a constant viscosity with respect to shear rate. A non-Newtonian fluid can either experience shear-thinning (more common) in which the viscosity decreases as shear rate increases, or shear-thickening in which viscosity increases as shear rate increases (less common). Due to the polymeric nature of fluids in nature, most biological fluids tend to exhibit non-Newtonian behavior.

## 2.2 Critical Dimensionless Parameters

### 2.2.1 Reynolds Number

The Reynolds number characterizes whether the inertial or viscous forces dominate in a flow.

The Reynolds number is defined as:

$$Re = \frac{\rho UL}{\mu} = \frac{\text{inertial forces}}{\text{viscous forces}} \quad (2.1)$$

where  $\rho$  is the density of the fluid,  $U$  is the fluid velocity,  $L$  is the characteristic length scale, and  $\mu$  is the viscosity. The Reynolds number classifies flow regimes such that a flow with a small Reynolds number ( $Re \ll 1$ ), the viscous forces dominate while in high Reynolds or turbulent regimes ( $Re \gg 1$ ), inertial forces dominate and viscous effects can be neglected.

### 2.2.2 Deborah Number

For viscoelastic fluids it is important to know how fast the time scale is over which the event is observed compared to the internal relaxation time of the fluid. The relaxation time,  $\lambda$ , is unique to viscoelastic fluids and physically describes how fast it takes the fluid to return to an equilibrium position. The Deborah number describes the ratio of this relaxation time to the characteristic time of the flow:

$$De = \frac{\lambda}{t_{char}} \quad (2.2)$$

The characteristic time  $t_{char}$  is dependent on the actual flow set-up; however, it generally describes the timescale over which an important kinematic event occurs, such as the time for the flow to pass over an object. It should be noted that for a given system there might be more than one critical time scales. Similar to the way in which large and small Reynolds numbers determine turbulent and laminar flow regimes, the magnitude of the Deborah number also

classifies flow regimes. In the limit where  $De \rightarrow 0$ , the fluid behaves like a Newtonian fluid. Conversely, when  $De \rightarrow \infty$  the fluid instead behaves like a solid. Intuitively, in this limit the polymeric molecules do not have time to relax during the time frame of the experiment such that the fluid acts as if it were an elastic solid. When the relaxation time and the characteristic time are approximately equal, or  $De \approx 1$ , the fluid will first exhibit noticeably non-Newtonian behavior.

### 2.2.3 Weissenberg Number

For systems with more than one characteristic time scale the Weissenberg number is another dimensionless group that characterizes the non-Newtonian behavior of the flow. Like the Deborah number it uses the relaxation time  $\lambda$  but it instead compares it to the strain rate:

$$Wi = \dot{\gamma}\lambda \tag{2.3}$$

where  $\dot{\gamma}$  is the shear fluid shear rate. The Weissenberg number can be thought of as a dimensionless shear rate. Like the Deborah number, large Weissenberg numbers indicate significant non-Newtonian behavior in the fluid, while small Weissenberg numbers ( $Wi < 1$ ) imply that the fluid behaves more Newtonian. However, the Deborah number is limited in the sense that it only accounts for the characteristic time of the flow and neglects any potential interactions the flow has with objects in the flow field. The Weissenberg can account for interactions between the object and the flow with the strain rate and is therefore the most critical dimensionless group in this analysis.

## 2.3 Viscoelastic Model

Due to the molecular composition of viscoelastic fluids, complex behavior is exhibited on the macro-scale. The Maxwell model of viscoelastic behavior is a simple yet effective means of characterizing the macroscopic properties of a viscoelastic fluid. For a standard Newtonian fluid the shear stress can be described by

$$\tau_{yx} = -\mu\dot{\gamma}_{yx} \quad (2.4)$$

which is independent of time. Maxwell proposed the constitutive model for viscoelasticity

$$\tau_{yx} + \frac{\mu}{G} \frac{\partial \tau_{yx}}{\partial t} = -\mu\dot{\gamma}_{yx} \quad (2.5)$$

with a time dependence on the shear stress. The viscosity divided by the elastic modulus ( $\mu/G$ ) acts as the time constant and is renamed the relaxation time,  $\lambda$ , due to the exponential decay of the shear stress over time. This can be better illustrated by dividing the shear stress term into a shear stress due to the fluid  $\tau_{yx}^f$  and a shear stress due to the polymers  $\tau_{yx}^p$ . The shear stress due to the fluid can be described by the Newtonian relation in equation 2.4, while the polymeric shear stress is described by the homogeneous differential equation

$$\tau_{yx}^p + \lambda \frac{\partial \tau_{yx}^p}{\partial t} = 0 \quad (2.6)$$

which can be solved to obtain an exponential relation between time and the shear stress with a time constant  $\lambda$ . The two shear stresses can be added linearly to obtain equation 2.5 rewritten as

$$\tau_{yx}^f + \tau_{yx}^p + \lambda \frac{\partial \tau_{yx}^p}{\partial t} = -\mu\dot{\gamma}_{yx} \quad (2.7)$$

which incorporates the stress due to the fluid and the time dependent stress behavior due to the polymers.

# Chapter 3

## Experimental Methods

### 3.1 Experiment Design

In order to test whether or not a flag will flap under an induced flow, a polycarbonate annulus was constructed and placed on a turn table. In the annulus, a stationary flag (or rod) is placed in the center of the channel supported by above with a thin, rigid rod. An overview of the experimental setup can be seen in figure 3.1. The outer polycarbonate cylinder has a diameter of 25 cm, while the inner cylinder has a 13 cm diameter, creating a circular channel 12 cm wide and 10 cm tall. The flag is supported by a brass rod 1.15 mm in diameter which is vertically attached to a horizontal cantilevered beam. The flag is lowered into the annular channel and aligned such that it is equidistant to each wall. The turn table can run at variable speeds ranging from 0 to 1.4 rad/s such that the velocity of the fluid near the flag can reach a maximum of 8.4 cm/s.

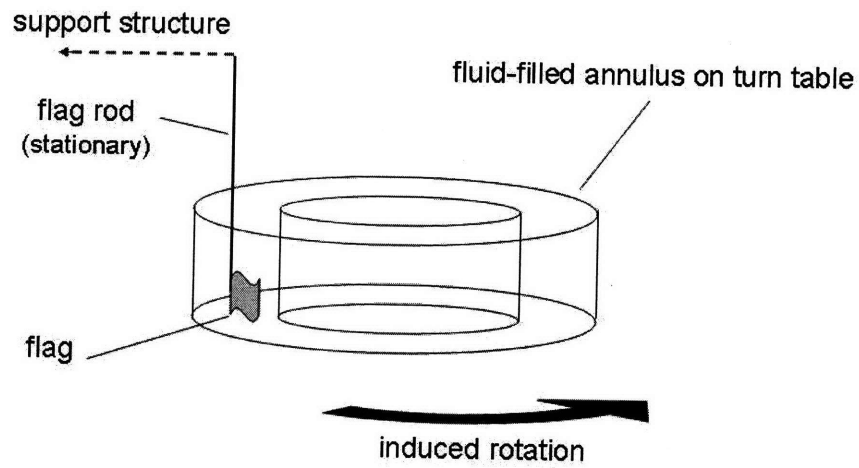


Figure 3-1: The experimental setup consists of a stationary flag subjected to a flow by a rotating annulus. As the rotation rate is controlled, the motion of the flag in the flow is observed.

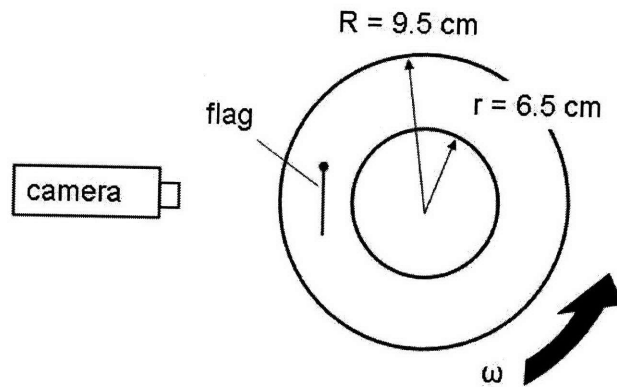


Figure 3-2: An overhead schematic of the experimental setup.

## 3.2 Fluids Tested: Properties and Structure

Two different fluids were tested with the flag: xanthan gum and micellar fluid. Both fluids used exhibited non-Newtonian behavior. The composition and structure of each fluid is described below.

### 3.2.1 Xanthan Gum

The xanthan gum polysaccharide is produced from the bacterium *Xanthomonas Campestris* and is most often used as a food additive. It has a large molecular weight on the order of  $5 \times 10^5$  g/mol and its chemical structure can be seen in figure 3.2.1. The xanthan gum solution used in this experiment was constructed based on Gicquel's report [3, 5]. It contains 0.1% xanthan gum in a 95:5 by weight glycerol and water solution for a total of approximately 3 L of solution. The solution was mixed by first taking 1.55 g of xanthan gum and mixing it into 0.199 L of distilled water to obtain a homogenous solution. This mixture was then added to 3 L of glycerol and mixed using an electric mixture until the xanthan gum solution is well incorporated. As this point, air bubbles have accumulated in the solution due to the mixing and the solution is left out overnight to degas. The xanthan gum solution, whose density is  $1.27 \text{ g/cm}^3$  has a relaxation time on the order of 27 seconds [5].

### 3.2.2 Micellar Fluid

Surfactants described a set of organic compounds which when added to aqueous solutions, lower the surface tension. Surfactant molecules are unique in the sense that they contain both a hydrophobic and hydrophilic group making them soluble in water and non-aqueous, hydrophobic solutions. Depending on the concentration of the surfactant, the molecules will assemble themselves in different arrangements. At low concentrations, small spherical micelles will form which as the concentration increases will grow into cylindrical, worm-like

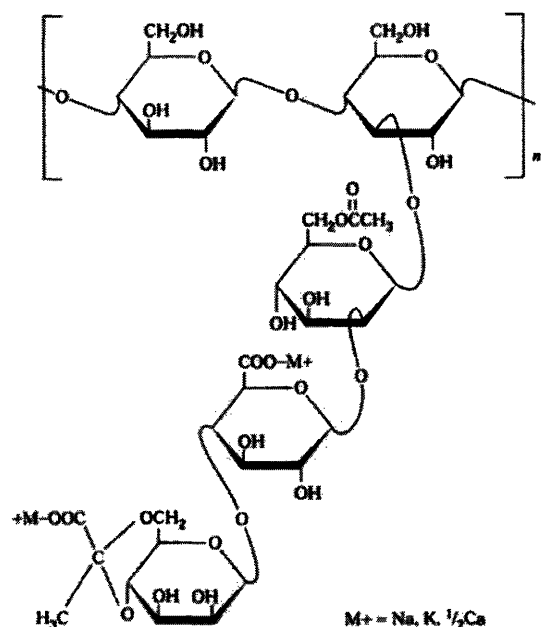


Figure 3-3: The molecular structure of the xantham gum polysaccharide [3]

micelles [2]. In aqueous solutions, these micelles form such that the hydrophilic heads are on the outside in contact with the fluid while the hydrophobic tails on the inside of the structure. When the worm-like micelles reach a sufficient length, they become flexible and act like polymers. How these “polymer” chains then interact depend on the concentration of the surfactant as is seen in figure 3.2.2.

The micellar fluid in this experiment uses the surfactant cetyl pyridinium chloride (CPyCl) mixed in a two to one concentration with the salt sodium salicylate (NaSal) in an equimolar brine solution. To create about one liter of the solution 1 L of distilled water is first mixed with 5.844 g of NaCl to form the brine. To the brine, 8.005 g of NaSal is added followed by 34.000 g of CPyCl. The solution is then continually mixed until it is homogeneous which is on the order of one day.

The shape of the micelles are very sensitive to changes in temperature, therefore the fluid

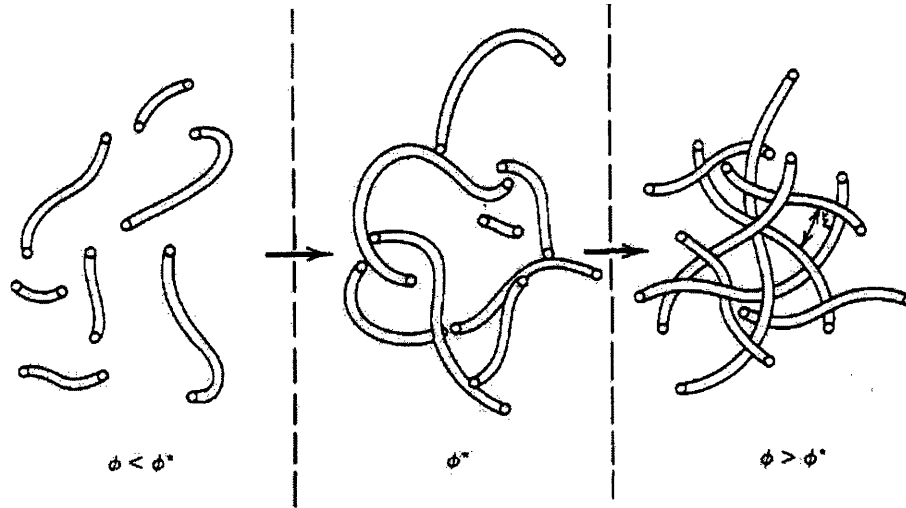


Figure 3-4: As the volume fraction of the surfactant molecule increases, the state of the solution changes [2]

Table 3.1: CPyCl/NaSal Fluid Properties at Varying Temperatures

Temperature ( $^{\circ}\text{C}$ )	Viscosity (Pa·s)	Relaxation Time (s)
20	30.9	1.2
21	24.9	1.0
22	19.8	0.8
22.5	17.7	0.7
23	16.05	0.6
24	12.9	0.5

properties also change dramatically over a small range of temperatures. The properties of the CPyCl/NaSal micellar fluid can be seen in table 3.1 (courtesy of Matthieu Varagnat) for environments close to room temperature. It should be noted that this experiment was conducted in a room at  $24^{\circ}\text{C}$  which corresponds to a relaxation time  $\lambda$  of 0.5 seconds and a dynamic viscosity  $\nu$  of  $12.9 \text{ m}^2/\text{s}$ .

### 3.3 Flag Material and Composition

The flag used in this experiment was fabricated using Zhermack's Elite Double 8 and made according to the manufacturer's instructions. The material itself is vinyl polysiloxane. It is

a highly elastic material with a Young's Modulus of 1.2 MPa and a density of  $1.4 \text{ g/cm}^3$ . The flag geometry was that of a long rod 1.15 mm in diameter and 60.18 mm long.

In addition to the vinyl polysiloxane rod, a mylar sheet  $15 \text{ }\mu\text{m}$  thick was tested (although only in the xanthan gum). Mylar is a significantly stiffer material with a Young's Modulus on the order of 4GPa. The mylar flag tested had a rectangular cross sectional area measuring about 30 mm by 60 mm.

### 3.4 Experimental Procedure

In order to observe the potential flapping behavior of the rod and flag, the fluid-filled annulus (see figure 3.4) was rotated at varying angular velocities while video imaging was used to capture the movement of the flag. For consistency, the following procedure was used:

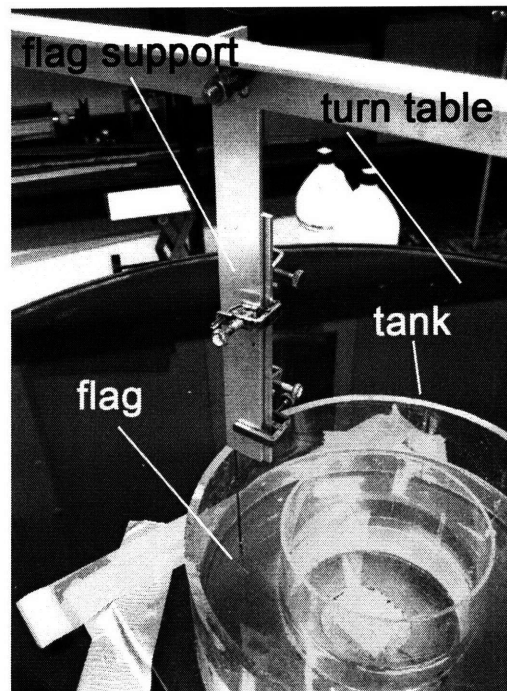


Figure 3-5: Image of the experimental setup.

1. The flag is centered in the channel of the annulus and placed at a specified height from

the bottom of channel as to avoid surface effects.

2. The video camera is set to record the flag and will remain in the same position for the duration of the experiment.
3. With the fluid of interest placed in the channel, the turn table is turned on to rotate at close to the maximum speed.
4. The turn table is allowed to run for five minutes to allow for a steady-state to be reached.
5. The flag is the recorded for four rotations of the tank.
6. The rotational rate is then lowered on the order of 0.2 rad/s and another five minutes is waited to allow for a new stead-state.
7. Steps 5 and 6 are repeated until the flapping is no longer observed or the turn table reaches its minimum velocity.
8. For continuity, steps 5 and 6 are repeated again, however increasing the rotational speed of the annulus until the maximum velocity of the turn table is reached.
9. The experiment is then stopped and appropriate scaling measurements are taken for the purpose of image analysis.

With the data taken, image analysis is performed to extract the frequency and amplitude of the oscillations. To verify the analysis, rough estimates of the frequency and amplitude are taken by eye using the video and compared to the computational results.

# Chapter 4

## Results and Discussion

### 4.1 Experimental Geometry and Dimensionless Groups

With the experimental setup set, the Deborah number (2.2) and the Weissenberg number (2.3) may be redefined according to the system's geometry. For two concentric, rotating cylinders, the Deborah number is defined by the angular velocity,  $\omega$ , of the cylinders [1]:

$$De = \lambda\omega \tag{4.1}$$

It should be noted that the Deborah number has no reference to the actual flag in the system, but is only characterizes the flow. The Weissenberg number also allows the placement of the flag to be taken into account. Since the shear rate is defined as:

$$\dot{\gamma} = \frac{\partial v_x}{\partial y}$$

with  $v_x$  as the velocity of the fluid in the direction of the rotation and  $y$  as the direction perpendicular to the rotation, for the purpose of dimensional analysis, we can approximate

the velocity gradient as linear

$$\dot{\gamma} \sim \frac{U}{H} = \frac{\omega R}{H}$$

where  $R$  is the distance from the center to the flag and  $H$  is distance from the flag to the closest wall or boundary, allowing our Weissenberg number to be redefined for our geometry:

$$Wi = \frac{\lambda \omega R}{H} \quad (4.2)$$

Although both dimensionless groups describe the magnitude to which the fluid behavior can be classified as non-Newtonian, since the Weissenberg number incorporates the interaction between the flag and the flow, it will be the primary number used in the analysis to characterize flow regimes.

## 4.2 Experimental Range of Parameters

Using the experimental procedure documented above, a range of angular velocities ranging from 0 to 1.5 rad/s can be tested. With the given experimental setup, this corresponds to fluid speeds of 0 to 28.5 cm/s near the flag. The flag was tested at two heights from the bottom of the tank: 1.5 cm and 2.5 cm which correspond to a maximum Weissenberg number of 13.3 and 8.0 respectively in the micellar fluid ( $\lambda$  of 0.5 s at 24°C). In the xanthan gum, which has a relaxation time of 27 s, the maximum experimental Weissenberg number increases to 513 for a flag placed 1.5 cm from the bottom of the tank. The Deborah numbers for each fluid can also be calculated. The maximum Deborah numbers for this experimental set up are 1.05 for the micellar fluid and 40.5 for the xanthan gum.

### 4.3 Flapping Image Analysis

A video recording was taken of the flapping flag using the standard 30 frames per second at a resolution of 640 by 480 pixels. The camera was placed in the same vertical plane as the flag and set to record perpendicular to the flag and the fluid flow. Using this method, flapping in the vertical direction could be detected by the images. To extract the frequency of the flapping, the video, transformed into a series of image files, was analyzed with matlab. The code to perform the analysis can be found in the appendix, the methodology is outlined here:

1. Create a mask of the baseline image excluding the flag.
2. Subtract the mask from each successive image to extract the flag and convert to black and white.
3. Find the boundary of the flag and the mean axis.
4. Use a fast fourier transform (FFT) to deduce the different frequencies from the movement of the mean axis between frames.

The peak frequency obtained from the FFT was also compared against a frequency estimate by observation of the video to ensure that the FFT analysis was in the correct range.

There are inherent problems with using video techniques to analyze the flapping motion of the flag. One potential problem is the diffraction by looking at the video through the curved, acrylic cylinder and fluid. To ensure that the flapping observed in the images was due to true motion of the flag and not a virtual movement, a larger object was placed in a flow with water. The image was then recorded and no movement was observed either in the video which validates that the flapping of the flag in the viscoelastic fluid was not an optical illusion.

The second issue that arose in regards to the recording was to ensure that the flapping is adequately expressed in the two-dimensional image on the video. The rod is not limited to flapping vertically, and because it is unconstrained, it can flap in the direction parallel to the camera such that the flapping is not projected onto the frame. Additionally, if the flapping occurs in some plane not exactly perpendicular to the camera, the flapping projected onto the image will be lesser in magnitude to the actual oscillation amplitude. To control for this the flag was placed as close to the bottom of the annulus as possible and equidistant from each of the cylindrical walls such that the dominating shear force would be from the bottom of the channel, minimizing the lateral effects.

## 4.4 Flapping Behavior in Xanthan Gum and Micellar Fluid

The experiment was performed with both xanthan gum and micellar fluid; however, no flapping behavior was observed with the xanthan gum with either the thin sheet of mylar or the vinyl polysiloxane rod. With the micellar fluid, flapping behavior was observed with the rod oscillating at angular velocities greater than about 0.2 rad/s. Figure 4.4 shows the movement of the rod in micellar fluid at a rotation rate of 1.25 rad/s. It can be seen that the majority of the flag remains in the same position while only the tail end of the flag flaps. The flapping appears to come in two modes, one which is a tail displacement and the other which is a change in curvature of the latter half of the flag. Moreover, although this image series only shows about 0.3 s, the flag does not have a clearly defined motion where it always returns to its singular equilibrium position in a prescribed amount of time. Instead, there is a range of positions over which it oscillates.

It is interesting to note that although the flow with the xanthan gum had the larger Weissenberg number, no flapping was observed. This implies that there may be inherently

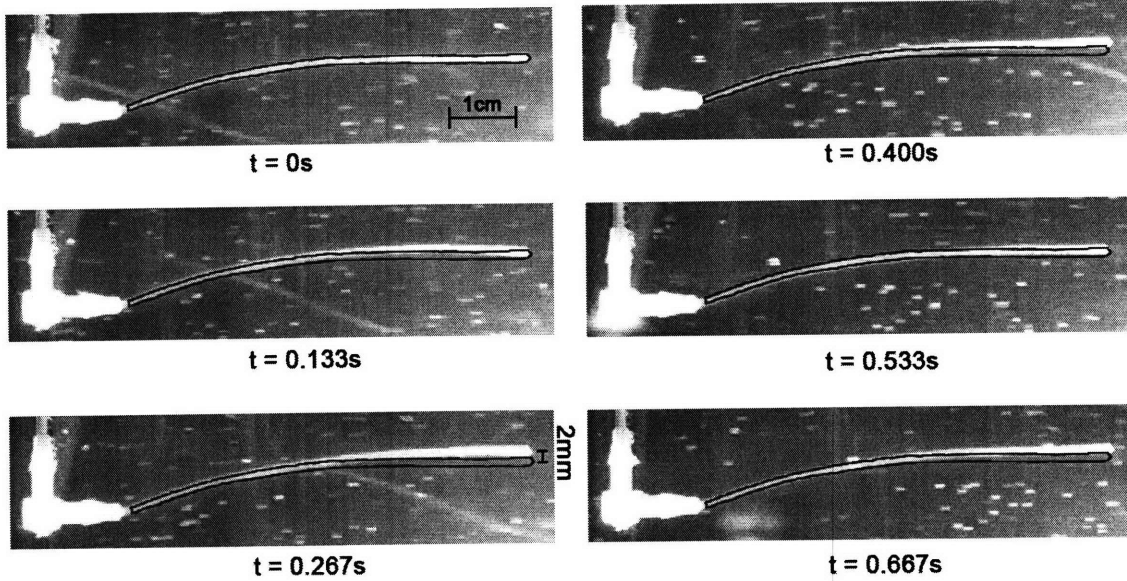


Figure 4-1: Image sequence of the flag in a flow of 1.2rad/s. The red outline notes the position of the flag in the first frame.

more complex behavior at the molecular level not accounted for in this model, since the chains of micelles in the CPyCl fluid may behave differently than ordinary polysaccharides.

## 4.5 Flapping Frequencies in Micellar Fluid

In the micellar fluid, the rod flaps not at a single frequency for any given rate of rotation. Figure 4.5 displays the highest frequency of the rod according to the rotational frequency of the annulus for the flag placed both 1.5 cm and 2.5 cm from the bottom of the tank. Although both sets of data are linear with respect to the Weissenberg number, the linear regression lines have different slopes and intercepts. Whereas the flag placed 2.5 cm from the bottom stops flapping with a  $Wi \sim 0.5$ , the other case would only flap if  $Wi > 2$ . Further work is needed to understand what the minimum Weissenberg number is such that flapping is observed in various fluids.

The rate of displacement of the tip of the flapping rod subjected to different speed flows can be seen in figure 4.5. As the figure indicates, the flag flaps without one clearly

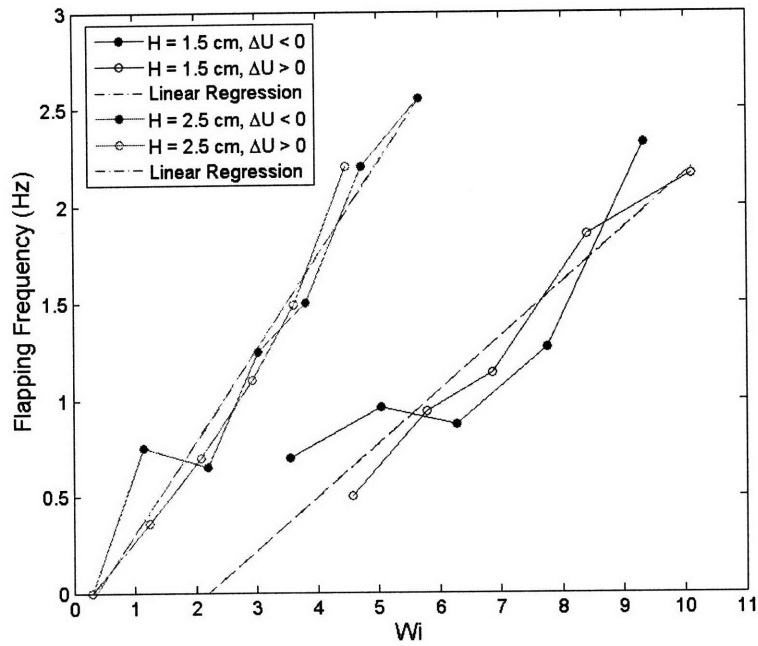


Figure 4-2: As the Weissenberg number increases there is a clear linear relation with the flapping frequency.

defined frequency; however the frequency of oscillation does increase with an increasing rate of rotation. In order to extract the dominant frequency in the flapping rod, fast Fourier transform (FFT) is used to obtain the result displayed in figure 4.5. Additionally this highest frequency was confirmed by visual image observation. From this analysis, the main trend shows that as the rotational frequency of the annulus increases, so does the flapping frequency. Intuitively, at these larger rotational frequencies, the larger Weissenberg numbers entail a larger shear stress acting on the flag causing an increase in the flapping.

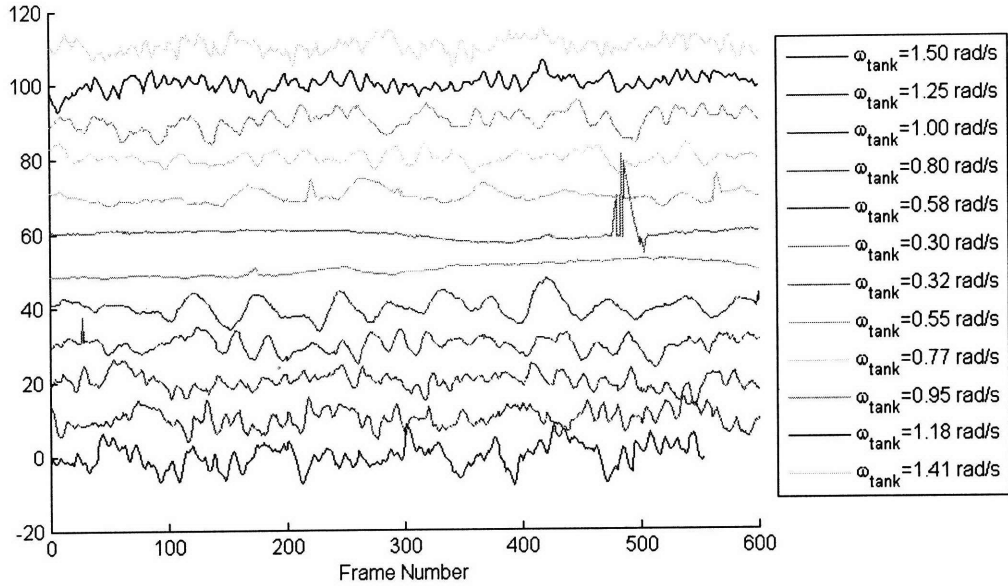


Figure 4-3: For a flag placed 2.5 cm from the bottom of the channel, as the rate of rotation increases, so does the rate at which the tip of the flag is displaced.

## 4.6 Bending Number: Dimensional Analysis of the Flapping

Since by nature problems dealing with viscoelastic fluids are inherently complex, for a first approximation we can look at dimensional analysis. On the flag there are two competing forces: the viscous drag from the fluid and the elasticity in the flag due to the material. Intuitively one expects that the more elastic the flag is, the more energy it can absorb from the fluid and the less it flaps. Conversely, the stiffer a flag is, less energy will be absorbed by the material and instead the energy will be dissipated through flapping. In the limit of small deflection of a rod, the bending force per unit length on the flag body can be expressed as [4]:

$$\frac{dF_B}{ds} \simeq \frac{dF_B}{dx} = B\partial_{xxxx}h \quad (4.3)$$

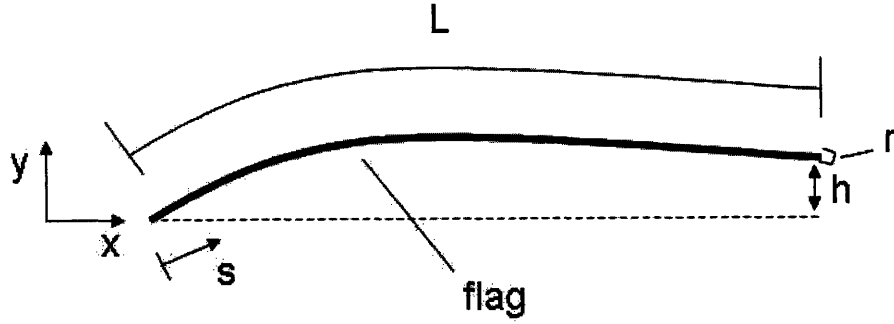


Figure 4-4: Schematic showing the critical parameters on the flag.

where  $B$  is the bending stiffness and can be expressed by the Young's Modulus of the flag material and the bending moment of inertia,  $B = EI$ . For the geometry of the flag, a beam with a circular cross section,  $I \sim r^4$ . Figure 4.6 gives an overview of the critical geometric parameters of the flag. The term  $\partial_{xxxx}h$  is the second derivative of curvature or the fourth derivative of the vertical displacement with respect to the horizontal position. The bending force in the flag needs to be balanced by the viscous force in the fluid:

$$\begin{aligned} \frac{dF_f}{ds} &\simeq \int \sigma(r d\theta) \\ &\propto \int \partial_x h \sigma_{xy} r d\theta \end{aligned}$$

where  $\sigma_{xy}$  is the shear stress in the fluid and is give by

$$\sigma_{xy} = \mu \dot{\gamma}$$

Equating the bending force in the flag and the viscous force in the fluid yields:

$$EI \partial_{xxxx} h \sim \partial_x h \mu \dot{\gamma} r$$

which has scaling like:

$$Er^4 \frac{h}{L^4} \sim \mu \dot{\gamma} \frac{h}{L} r$$

The ratio of the two sides gives the appropriate dimensionless number showing the ratio of the viscous drag and the bending force:

$$\text{Bending Number} = \frac{\text{viscous drag}}{\text{bending force}} = \frac{\mu \dot{\gamma} L^3}{Er^3} \quad (4.4)$$

For the range of experiments tested in this paper, the bending number was on the order of  $10^2$  for the micellar fluid. In other words, the force due to the viscous drag of the fluid was 100 times greater than the elasticity in the flag. For the flag places in xanthan gum, which did not flap, this ratio was on the order of 10.

In addition to the ratio of viscous drag and internal elastic forces, it is also useful to quantify the ratio of the elastic force of the fluid to the elasticity of the flag body. Through dimensional reasoning, the Weissenberg number can be thought of as the ratio of viscous stress ( $\mu \dot{\gamma}$  with units of [Pa]) to elastic stress ( $\mu/\lambda$  with units of [Pa]) in a fluid. Therefore, by dividing the bending ratio in (4.4) by the Weissenberg number, the viscous forces in the fluid cancel to obtain a ratio between the elastic forces in the fluid to the elastic force in the flag body which is now independent of the shear rate. For the flag geometry and material used, for the micellar fluid this number was on the order of 25 with the elastic forces in the fluid dominating. Conversely for the xanthan gum this ratio was on the order of 0.05 with the elastic forces in the flag dominating. This difference between the xanthan gum and micellar fluid elastic ratio implies that among other conditions, in order for flapping to occur the elastic forces in the fluid must dominate over the elastic force in the body.

## 4.7 Frequency Dimensional Analysis

In order to obtain the scaling for the flapping frequency, dimensional analysis can be used again. Starting with Newton's second law, the inertia force per unit length on the flapping flag has a dimension of

$$\frac{dF_I}{ds} \approx \frac{d}{dx}(\rho \partial^2 y / \partial t^2) \sim \rho h / L \tau^2 \quad (4.5)$$

where  $\tau$  is the time scale of flapping for a flag flapping with frequency  $\omega$  and oscillation amplitude  $h$ . Additionally the external force acting on the body is from the shear stress in the fluid such that

$$\frac{dF_I}{ds} \approx \int \sigma_{yy} r d\theta \sim Wi \mu \partial_y v_y r \sim Wi \mu r / \tau \quad (4.6)$$

where  $r$  is the radius of the rod and the stress scales with the Weissenberg number. The time scale ( $\tau$ ) is set to  $1/\omega$  for the flapping flag. By balancing bending and inertia forces, one gets

$$\omega \sim \frac{\mu r L}{\rho h} Wi \propto Wi \quad (4.7)$$

which more generally shows that the frequency is directly proportional to the Weissenberg number. This linear relation between the frequency and the Weissenberg number is confirmed by the experiment; however, it does not account for the different slopes in figure 4.5. Additionally because the viscosity  $\mu$  in (4.7) is not the viscosity for the fluid but rather the polymer viscosity, it is difficult to experimentally determine and no direct comparison between this analytical approximation and the experimental results displayed in figure 4.5 can be obtained.

# Chapter 5

## Future Work

Future work to explore the flapping of flag-like objects in viscoelastic fluid should focus first on improving the experimental set up as well as performing a variety of more tests to explore different materials, fluids, and flow regimes. The experiment documented by this paper used a rotating annulus to induce a flow. However, even for the length of the flags tested, they exhibited curving to match the circular shape which may have had an effect on the amplitude or frequency of oscillation observed. Moreover, it was difficult to center the flag in the annulus. By creating a setup where the flag lies in a linear channel and fluid is circulated through will minimize the above difficulties.

Additionally, due to the discrepancy in flapping between the micellar fluid and the xanthan gum, the experiment should be performed again with xanthan gum in a similar range of Weissenberg numbers as the micellar fluid. As long as the flag experiences the same invariant flow condition, the flag should flap regardless of the actual flow parameters. To test a range of dimensionless conditions, a variety of materials should be used to construct different flags as well as flags in different geometries, such as a rectangular plane in addition to the rod. Other fluids should also be used to determine whether or not the flapping is a function of the molecular structure instead of merely macroscopic parameters.

# Chapter 6

## Conclusion

Subject to a flow in a viscoelastic fluid, it is possible for a flag-like object to exhibit flapping. Under the proper conditions, this experiment proved that a slender polysiloxane rod can flap when placed in a flow of a cetyl pyridinium chloride micellar fluid but not in a xanthan gum solution. Figure 6 summarizes under which flow conditions flapping occurred or did not occur. Regardless of the fluid speed tested in this experiment, the flag did not flap under the xanthan gum where the elastic forces in the flag dominated the elastic forces in the fluid unlike with the micellar fluid. It is posed that if the conditions could be changed such that this ratio favored the elastic forces in the fluid over the flag, a flag could flap under the proper parameters in xanthan gum.

The flapping of the flag under specific flow conditions in a viscoelastic fluid has implications in biological swimming applications, especially in that of sperm and other flagellum-propelled organisms, since the majority of biological fluids are viscoelastic. Hyperactivated sperm placed in a viscous, viscoelastic fluid adapt by altering their swimming dynamics. Instead of sinusoidal-like wave, they produce an irregular wave at the tip of the flagella to propel themselves. This study shows that in such a fluid environment, the energetically favorable motion of a slender rod, such as a flagella, is to flap by displacing the tail end of

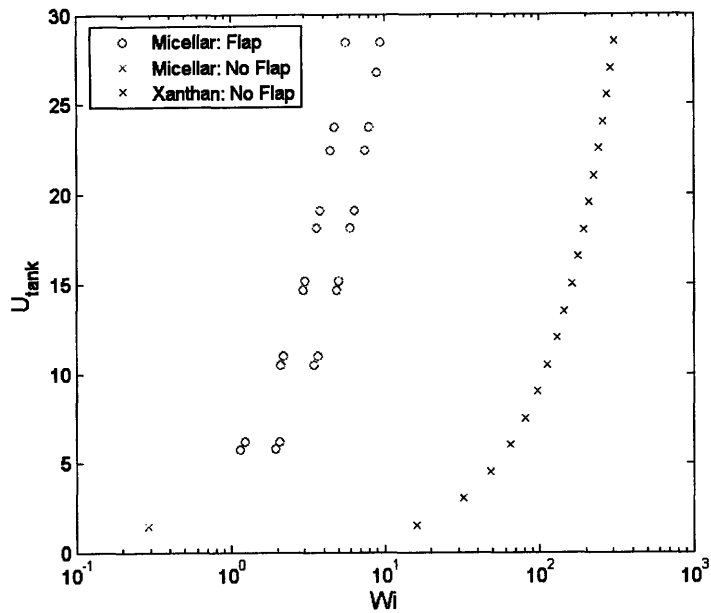


Figure 6-1: Flapping was observed in the micellar fluid over a range of Weissenberg numbers, however no flapping was observed in the xanthan gum in this experiment.

the rod while the majority of the remains fixed in place. Although this study only observes the passive case of a rod in a viscoelastic fluid flow, the results are promising for future work in the field. Additional work can focus not only on changing the parameters of the fluid and the flag, but also applying this concept to the active case where the flag is given an input wave and the output waveform under the viscoelastic flow is observed.

# Bibliography

- [1] R. Byron Bird, Robert C. Armstrong, and Ole Hassager, *Dynamics of polymeric liquids*, 2 ed., vol. 1, Wiley, 1987.
- [2] ME Cates and SJ Candau, *Statics and dynamics of worm-like surfactant micelles*, J. Phys.: Condens. Matter **2** (1990), 6869–6892.
- [3] M Gicquel, *A viscoelastic fluid to beat the scallop theorem: Can a one-hinged organism swim in a viscoelastic fluid?*, Tech. report, cole Polytechnique, 2007.
- [4] AE Hosoi and L Mahadevan, *Peeling, healing, and bursting in a lubricated elastic sheet*, Phys. Rev. Lett. **93** (2004), no. 13, 13.
- [5] LB Smolka and A Belmonte, *Charge screening effects on filament dynamics in xanthan gum solutions*, J. Non-Newtonian Fluid Mech. **137** (2006), 103–109.
- [6] SS Suarez and H-C Ho, *Hyperactivated motility in sperm*, Reprod. Dom. Anim. **38** (2003), 119–124.
- [7] GI Taylor, *Analysis of the swimming of microscopic organisms*, Proceedings of the Royal Society of London. Series A, Mathematical and Physical Sciences **209** (1951), no. 1099, 447–461.